Energy Conversion and Management 89 (2015) 244–250

Contents lists available at ScienceDirect

Energy Conversion and Management

journal homepage: www.elsevier.com/locate/enconman

Theoretical analysis on the performance of annular thermoelectric couple

Zu-Guo Shen, Shuang-Ying Wu *, Lan Xiao

Key Laboratory of Low-Grade Energy Utilization Technologies and Systems, Ministry of Education, Chongqing University, Chongqing 400044, China
College of Power Engineering, Chongqing University, Chongqing 400044, China

ARTICLE INFO

Article history:
Received 28 April 2014
Accepted 28 September 2014

Keywords:
Annular thermoelectric couple
Annular shaped parameter
Efficiency
Dimensionless output power
Theoretical analysis

ABSTRACT

For round shaped heat source or heat sink, the annular thermoelectric couple (ATEC) with annular shaped legs instead of flat-plate thermoelectric couple (FTEC) is proposed to solve the performance deterioration caused by geometries mismatching. Based on one-dimensional steady model, the fundamental formulas of ATEC are derived. The impact of geometric feature of ATEC manifested by the annular shaped parameter s_r, on the dimensionless output power and efficiency of ATEC under different temperature ratios, external loads and dimensionless figure of merits is examined theoretically. Also, to enhance the practicability of ATEC, some suggestions or notes are provided. Results show that the forms of fundamental formulas about ATEC are the same as those about FTEC. Compared to temperature ratio and dimensionless figure of merit, the influence of s_r is affected by external load seriously. The extremums of dimensionless output power and efficiency are presented on condition that $s_r = 1$. As the closer s_r is to 1, the larger the dimensionless output power is. In view of this behavior, a new structure including an additive material with high thermal conductivity is designed for recovering cost-free energy resources with ATEC.

1. Introduction

As a result of energy crisis and environmental pollution followed by immoderately burning fossil fuels in recent several decades, many efforts have been poured into the researches of renewable clean energy resources. Thermoelectric power generation, because of its simplicity, less maintenance cost, high reliability and environmental friendliness, has become a promising clean energy conversion technology. However, due to the relatively low thermal-to-electric efficiency compared to conventional power generation technologies [1], the commercialization of this technology is limited, mainly in the fields of low cost or cost-free energy resources, such as solar energy [2–4] and waste heat from automotive exhaust gases [5,6].

The performance of thermoelectric generator (TEG) composed of a series of thermoelectric couples is directly related to the dimensionless figure of merit (*ZT*), geometric arrangement of thermocouple, external load and temperatures of cold and hot junctions. To increase the competitiveness of thermoelectric power generation technology, extensive investigations have been conducted.

Considerable improvement about *ZT* was obtained in recent decades. Zhao et al. [7] reported a *ZT* of 2.9 at 923 K in SnSe single crystals, which was the highest up to present. By introducing shape parameter, Sahin and Yilbas [8] and Ali et al. [9] investigated the effect of leg geometry on the performance of thermoelectric couple. Ref. [8] showed that the efficiency of thermoelectric couple increased notably when the leg geometry became a trapezium shape along the leg height. Optimal external load for peak power of a TEG in solar application was carried out by Lesage et al. [10] using two experimental apparatuses. They indicated that the load matching condition cannot yield peak power for any of the thermal conditions tested. Also, a simplified normalized power relation was put forward.

The temperatures of cold and hot junctions were determined by heat transfer capabilities between TEG and heat source or heat sink. Some appropriate approaches for increasing heat transfer capabilities were proposed and investigated. In detail, Crane and Jackson [11] created a numerical model and studied an integrated thermoelectric cross flow heat exchanger. Based on theoretical and experimental studies, some suggestions for performance improvement of TEG were proposed by Gou et al. [12], such as expanding heat sink surface area in a proper range and enhancing cold-side heat transfer capacity in a proper range. The performance of TEG at various operating conditions was studied experimentally by Chen et al. [13]. Results showed that the effects of flow pattern

* Corresponding author at: College of Power Engineering, Chongqing University, Chongqing 400044, China. Tel.: +86 (0)13657693789; fax: +86 23 65102473.
E-mail address: shuangyingwu@126.com (S.-Y. Wu).

http://dx.doi.org/10.1016/j.enconman.2014.09.071
0196-8904/

Nomenclature

A	cross-section area of leg, m^2
I	electrical current, A
k	thermal conductance of leg, W/(m K)
K	overall thermal conductance of ATEC, W/(m K)
P	output power of ATEC, W
Q	heat flow rate, W
Q_{in}	Fourier heat input, W
Q_{out}	Fourier heat output, W
Q_J	Joule heat, W
r	radial direction
R	total electrical resistance of ATEC, Ω
R_L	external load, Ω
s_r	annular shaped parameter
T	temperature, K
T_m	average temperature, K
ZT_m	the dimensionless figure of merit

Greek symbols

α	Seebeck coefficient, V/K
λ	thermal conductivity of leg, W/(m K)
σ	electrical conductivity of leg, Ω^{-1} m^{-1}
$\Delta\varphi$	angle in the direction of circumference, rad
δ	thickness of leg, m
θ	dimensionless temperature ratio
η	efficiency of ATEC

Subscripts

n	n-type leg
p	p-type leg
0	reference position
1	hot junction
2	cold junction

of heat sink and water flow rate were not significant, but the heat source temperature played an important role. Love et al. [14] investigated the influences of heat exchanger material and fouling on TEG exhaust heat recovery. They pointed out that the performance of thermoelectric device with stainless steel heat exchanger was lower than that with aluminum heat exchanger due to the difference of thermal conductivity, and heat exchanger fouling can degrade the performance of studied devices. Using exhaust gas of vehicles as heat source, a mathematical model for the performance of TEG devices was developed by Wang et al. [15]. The findings revealed that the benefit caused by changing the convection heat transfer coefficient of high-temperature side was more pronounced than that of low-temperature side. The power output characteristics of TEG with plate-fin heat absorber were investigated by Jang et al. [16] using three-dimensional numerical method. Results indicated that the optimal fin height and flue gas velocity existed for maximizing net power density. In the experiment conducted by Lesage et al. [17], the effects of two flow channel inserts (panel and spiral inserts) strengthening the heat transfer coefficient on power generation of liquid-to-liquid TEG were considered. It was shown that the panel inserts enhanced power up to 110%, while the spiral inserts produced negligible power enhancement. Using the same experimental apparatus presented in Ref. [17], the net power output of TEG under various panel densities of flow impeding geometric inserts was explored by Amaral et al. [18]. Optimal insert panel density maximizing the net power was identified with respect to flow rate. A micro-TEG was proposed and its performance was researched by Wojtas et al. [19]. This device had the advantages of high heat transfer coefficient and small pumping power in a compact volume. Results suggested that the optimization for thermoelectric material should focus more on the power factor than on ZT itself when systems had good thermal coupling. Besides, Wang et al. [20] designed the geometry of heat sink such as fin spacing and length with two-stage optimization. Jang and Tsai [21] optimized TEG modules pacing and its spreader thickness using a simplified conjugate-gradient method. Tzeng et al. [22] discussed the configurations and dimensions of heat absorber and heat sink by applying one-dimensional steady model. Also, heat pipe [23,24] and thermosyphon [25] heat sink were employed in solar hybrid systems with TEGs to enhance heat transfer capability.

From Refs. [11–25], two features have been found. On one hand, all of them were limited to flat-plate thermoelectric couple (FTEC), where the cross-section shape of legs was flat-plate. On the other hand, almost all of these studies were concentrated on methods to increase heat transfer coefficient, which included altering flow patterns [13] and heat exchanger materials [14], adding flow channel inserts [17,18], applying micro fluidic heat transfer system [19], heat pipe [23,24] and thermosyphon [25]. However, in some practical applications, such as converting heat from automotive exhaust gases [5,26] and from coal-fired boiler [27], utilizing solar energy with heat pipe [23,24] or thermosyphon [25], the heat source or heat sink is cylindrical in shape. In these situations, if FTEC was still adopted, poor heat transfer capability caused by the relative geometries of heat source or heat sink and thermoelectric couple would be presented [10] in spite of taking above methods to increase heat transfer coefficient. Consequently, the performance of thermoelectric couple would be degraded and the commercialization of thermoelectric power generation technology would be further postponed. In this regard, annular thermoelectric couple (ATEC) with annular shaped leg is proposed, ascribing to the fact that ATEC can contact with heat source or heat sink closely showing much smaller heat transfer resistance than that of FTEC. Currently, the annular shaped thermoelectric module has already been fabricated [28]. Yet, to the best knowledge of authors, the study related to ATEC has received very little attention, and the impact of annular shaped parameter characterizing the feature of ATEC on the performance of thermoelectric couple is blank. What's more, considering the fact that non-constant cross-section along thermocouple leg and annular shape are presented in ATEC, some new behaviors may occur, such as the allocation of generated Joule heat on both junctions of ATEC. Thus the previous formulas preparing for FTEC may be inapplicable to ATEC.

In the present study, taking ATEC as object, the fundamental formulas of ATEC including temperature distribution along the legs, heat absorbed at hot junction and dissipated at cold junction, output power and efficiency, are derived based on one-dimensional steady model. Then the effect of annular shaped parameter on the performance of ATEC under different operating temperature ratios, external loads and ZT is theoretically analyzed. In the end, some suggestions or notes for practical applications of ATEC are provided.

2. Theoretical model

A typical ATEC is presented in Fig. 1, which consists of a p- and n-type thermoelectric legs sandwiched between heat source and heat sink. The first part of this study is to derive the fundamental formulas of ATEC. Fig. 2 shows the physical model of one leg. In

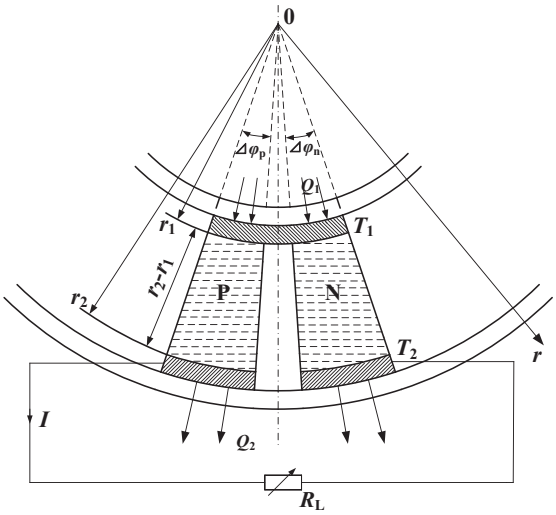

Fig. 1. Schematic view of a typical thermoelectric couple with annular geometric legs.

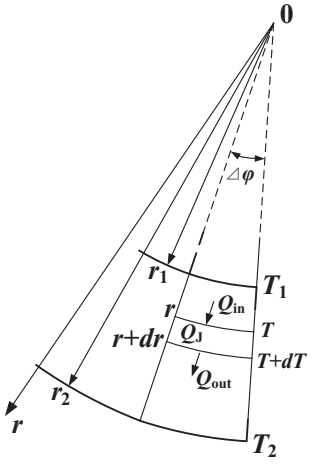

Fig. 2. A leg of ATEC for theoretical analysis.

the theoretical analysis, the following approximations are made [2,8,9]:

- The properties of leg material are independent to temperature and position, so the Thomson effect is neglected.
- The temperatures of hot and cold junctions are maintained at constant values of T_1 and T_2 respectively.
- Electric and thermal contact resistances are negligible.
- One-dimensional heat transfer along the radial direction r is considered, and the lateral surfaces are considered to be adiabatic.
- Along the leg (p- or n-type leg) height direction, the leg has the same thickness.

These assumptions allow us to focus on the fundamental information of ATEC. Applying energy balance to the infinitesimal element dr shown in Fig. 2, it has

$$Q_{in} + Q_J - Q_{out} = 0 \tag{1}$$

where Q_{in}, Q_{out} and Q_J are the Fourier heat input, Fourier heat output and generated Joule heat, respectively. Eq. (1) can be rewritten as

$$\lambda A(r)\frac{d^2T}{dr^2} + \lambda\frac{dA(r)}{dr}\frac{dT}{dr} + \frac{I^2}{\sigma A(r)} = 0 \tag{2}$$

where I is the current following through leg. λ, σ and T are the thermal conductivity, electrical conductivity and temperature of leg, respectively. $A(r)$ is the cross-section area of leg, which can be expressed as

$$A(r) = \Delta\varphi \cdot r \cdot \delta \tag{3}$$

Taking the area $A(r_0)$ in the position of $r_0 = (r_1 + r_2)/2$ as reference, $A(r)$ can be expressed as

$$A(r) = A(r_0)\frac{r}{r_0} \tag{4}$$

where $\Delta\varphi$ and δ are respectively the angle in the direction of circumference and thickness of leg. r_1 and r_2 represent the positions of hot and cold junctions of ATEC. Substituting Eq. (4) into Eq. (2), Eq. (2) can be reformed as

$$\frac{d^2T}{dr^2} + \frac{1}{r}\frac{dT}{dr} + \left(\frac{r_0}{r}\right)^2\frac{I^2}{\lambda\sigma}\frac{1}{A^2(r_0)} = 0 \tag{5}$$

According to the assumptions, the boundary conditions are

$$T(r = r_1) = T_1,\ T(r = r_2) = T_2 \tag{6}$$

To reduce the cost of manufacture, the geometric dimensions of p- and n-type legs are the same as Ref. [29], i.e., $A_p(r) = A_n(r) = A(r)$, $\Delta\varphi_p = \Delta\varphi_n = \Delta\varphi$, $\delta_p = \delta_n = \delta$, $r_{1p} = r_{1n} = r_1$, $r_{2p} = r_{2n} = r_2$. Hence, the temperature distributions of p- and n-type legs are similar and can be expressed respectively as

$$\begin{aligned} T_p(r) = &-\frac{I^2r_0^2}{2\lambda_p\sigma_pA^2(r_0)}(\ln r)^2 \\ &+\left[\frac{I^2r_0^2(\ln r_1 + \ln r_2)}{2\lambda_p\sigma_pA^2(r_0)} + \frac{T_1 - T_2}{\ln r_1 - \ln r_2}\right]\ln r \\ &+\frac{T_2\ln r_1 - T_1\ln r_2}{\ln r_1 - \ln r_2} - \frac{I^2r_0^2\ln r_1\ln r_2}{2\lambda_p\sigma_pA^2(r_0)} \end{aligned} \tag{7}$$

$$\begin{aligned} T_n(r) = &-\frac{I^2r_0^2}{2\lambda_n\sigma_nA^2(r_0)}(\ln r)^2 \\ &+\left[\frac{I^2r_0^2(\ln r_1 + \ln r_2)}{2\lambda_n\sigma_nA^2(r_0)} + \frac{T_1 - T_2}{\ln r_1 - \ln r_2}\right]\ln r \\ &+\frac{T_2\ln r_1 - T_1\ln r_2}{\ln r_1 - \ln r_2} - \frac{I^2r_0^2\ln r_1\ln r_2}{2\lambda_n\sigma_nA^2(r_0)} \end{aligned} \tag{8}$$

The heat transferred through the leg of ATEC along r is presented as

$$Q = -\lambda A(r)\frac{dT}{dr} \tag{9}$$

Rearranging Eq. (9) and performing integration, the following result can be obtained.

$$Q = \frac{\lambda\cdot\Delta\varphi\cdot\delta}{\ln(r_2/r_1)}(T_1 - T_2) \tag{10}$$

Thus the thermal conductance k of leg can be defined as

$$k = \frac{\lambda\cdot\Delta\varphi\cdot\delta}{\ln r_2 - \ln r_1} \tag{11}$$

The overall thermal conductance K of ATEC shown in Fig. 1 is

$$K = k_p + k_n = \frac{\lambda_p\cdot\Delta\varphi\cdot\delta}{\ln r_2 - \ln r_1} + \frac{\lambda_n\cdot\Delta\varphi\cdot\delta}{\ln r_2 - \ln r_1} \tag{12}$$

On the other hand, the total electrical resistance R of ATEC can be presented as

$$R = \int_{r_1}^{r_2} \left(\frac{dr}{\sigma_p A(x)} + \frac{dr}{\sigma_n A(x)} \right) = \frac{\ln r_2 - \ln r_1}{\sigma_p \cdot \Delta\varphi \cdot \delta} + \frac{\ln r_2 - \ln r_1}{\sigma_n \cdot \Delta\varphi \cdot \delta} \tag{13}$$

The heat absorbed at the hot junction Q_1 and dissipated at the cold junction Q_2 of ATEC are

$$Q_1 = (\alpha_p - \alpha_n) I T_1 - \left[\lambda_p A(r) \frac{dT_p}{dr} \right]_{r=r_1} - \left[\lambda_n A(r) \frac{dT_n}{dr} \right]_{r=r_1} \tag{14}$$

$$Q_2 = (\alpha_p - \alpha_n) I T_2 - \left[\lambda_p A(r) \frac{dT_p}{dr} \right]_{r=r_2} - \left[\lambda_n A(r) \frac{dT_n}{dr} \right]_{r=r_2} \tag{15}$$

where α_p and α_n are the Seebeck coefficients of p- and n-type legs respectively.

Now combining Eqs. (4), (7), (8), (12), and (13) with Eqs. (14) and (15), Q_1 and Q_2 become

$$Q_1 = \alpha I T_1 + K(T_1 - T_2) - 0.5 I^2 R \tag{16}$$

$$Q_2 = \alpha I T_2 + K(T_1 - T_2) + 0.5 I^2 R \tag{17}$$

where $\alpha = \alpha_p - \alpha_n$ is the Seebeck coefficient of ATEC. When the external resistance R_L is imposed on ATEC, the current I through it can be expressed as follows

$$I = \frac{\alpha(T_1 - T_2)}{R + R_L} \tag{18}$$

The output power P and efficiency η of an ATEC can be given as

$$P = Q_1 - Q_2 = \frac{\alpha^2 (T_1 - T_2)^2 R_L}{(R + R_L)^2} \tag{19}$$

$$\eta = \frac{P}{Q_1} = \frac{\alpha^2 (T_1 - T_2) R_L}{\alpha^2 T_1 (R + R_L) + K(R + R_L)^2 - 0.5\alpha^2 (T_1 - T_2) R} \tag{20}$$

As can be seen, the forms of Eqs. (16), (17), (19), and (20) are the same as those of FTEC with constant cross-section area [30]. And from the above derivation process, it can be concluded that for any types of thermoelectric couple (FTEC, ATEC or others) and cross-section geometries, the corresponding forms of Q_1, Q_2, P and η must be the same except for the expressions of K and R, provided that the mentioned assumptions are satisfied. It provides the theoretical basis for Refs. [8,9], where the source of formula about the efficiency of FTEC with non-constant cross-section is not given.

The dimensionless figure of merit ZT_m based on the average temperature $T_m = (T_1 + T_2)/2$ is provided as

$$ZT_m = \frac{\alpha^2}{KR} \cdot \frac{(T_1 + T_2)}{2} = \frac{\alpha^2 (\theta + 1) T_2}{2KR} \tag{21}$$

where θ is the dimensionless temperature ratio and defined as

$$\theta = T_1 / T_2 \tag{22}$$

The referenced thermal conductance K_0 and electrical resistance R_0 based on the position r_0 of n-type leg [8], respectively, can be expressed as

$$K_0 = \frac{\lambda_n \cdot \Delta\varphi \cdot \delta \cdot (r_1 + r_2)/2}{r_2 - r_1} \tag{23}$$

$$R_0 = \frac{r_2 - r_1}{\sigma_n \cdot \Delta\varphi \cdot \delta \cdot (r_1 + r_2)/2} \tag{24}$$

The annular shaped parameter s_r is defined as

$$s_r = r_2 / r_1 \tag{25}$$

Further assuming the similar doped alloys are used to make p- and n-type ATEC legs, so $\lambda_p = \lambda_n = \lambda$, $\sigma_p = \sigma_n = \sigma$, $\alpha_p = -\alpha_n = 0.5\alpha$ [29]. Combining this hypothesis with Eqs. (12), (13), and (23), (24), (25), the dimensionless forms of R and K can be obtained as

$$\frac{R}{R_0} = \frac{(s_r + 1) \ln s_r}{s_r - 1} \tag{26}$$

$$\frac{K}{K_0} = \frac{4(s_r - 1)}{(s_r + 1) \ln s_r} \tag{27}$$

Substituting Eqs. (21)–(24), (26), and (27) into Eqs. (19) and (20), the dimensionless forms of P and η, which are the implicit functions of s_r, can be written as

$$\frac{P}{K_0 T_2} = \frac{2(K/K_0)(ZT_m)(R_L/R_0)(R/R_0)(\theta - 1)^2}{(\theta + 1)[(R_L/R_0) + (R/R_0)]^2} \tag{28}$$

$$\eta = \frac{2(ZT_m)(\theta - 1)(R_L/R_0)(R/R_0)}{(\theta + 1)[(R_L/R_0) + (R/R_0)]^2 + 2\theta(ZT_m)(R/R_0)[(R_L/R_0) + (R/R_0)] - (ZT_m)(\theta - 1)(R/R_0)^2} \tag{29}$$

Equating the first partial derivative of Eq. (28) with respect to R_L to zero, R_L corresponding to the maximum output power can be obtained as follows

$$R_L = R \tag{30}$$

Eq. (30) agrees with Ref. [2]. Similarly, R_L for maximum efficiency, which is the same as that in Ref. [2], is given by

$$R_L = \sqrt{1 + ZT_m} R \tag{31}$$

Then the maximum dimensionless output power and efficiency of ATEC, respectively, are

$$\left(\frac{P}{K_0 T_2} \right)_{max} = \frac{(ZT_m)(K/K_0)(\theta - 1)^2}{2(\theta + 1)} \tag{32}$$

$$\eta_{max} = \frac{2(ZT_m)(\theta - 1)\sqrt{1 + ZT_m}}{(\theta + 1)\left(1 + \sqrt{1 + ZT_m}\right)^2 + 2\theta(ZT_m)\left(1 + \sqrt{1 + ZT_m}\right) - (ZT_m)(\theta - 1)} \tag{33}$$

According to Ref. [31], Eq. (33) can be further reformed as

$$\eta_{max} = \frac{\theta - 1}{\theta} \frac{\sqrt{1 + ZT_m} - 1}{\sqrt{1 + ZT_m} + 1/\theta} \tag{34}$$

Eqs. (32)–(34) clearly show that in ATEC, the maximum dimensionless output power is affected by s_r, whereas the maximum efficiency remains unchanged with varying s_r. Furthermore, the conclusion that the geometries of thermoelectric couple legs have no effect on the maximum efficiency can be inferred according to Eqs. (33) and (34).

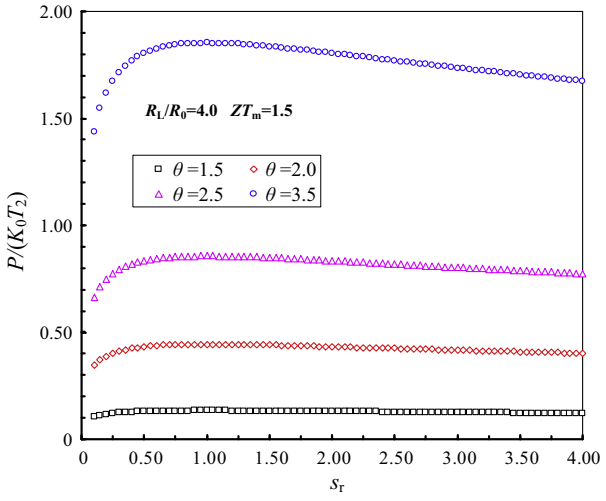

Fig. 3. Variation of $P/(K_0T_2)$ with s_r at different θ for $R_L/R_0 = 4.0$, $ZT_m = 1.5$.

It should be noted that $s_r < 1$ represents a kind of ATEC that the cold junction locates in the concave side, while the hot junction is placed in the concave side for $s_r > 1$ (like the situation shown in Fig. 1). ATEC is transformed into FTEC on the condition that $s_r = 1$, i.e., both r_1 and r_2 tend to be infinite. In this case, the derived formulas, like Eqs. (16) and (17), are the same as Ref.[30] totally, demonstrating that the above theoretical model is valid.

Due to the fact that the leg length of ATEC compared to r_1 or r_2 is relatively small, the considered range of s_r is between 0.1 and 4.0. Meantime, the following parameters are employed: $\theta = 2.0$, $R_L/R_0 = 4.0$ and $ZT_m = 1.5$.

3. Results and discussion

Under the conditions of different θ, R_L/R_0 and ZT_m, theoretical analysis of ATEC is conducted to examine the effect of s_r on $P/(K_0T_2)$ and η of ATEC. The leg length (r_2-r_1) and $\Delta\varphi$ are assumed to be constant.

Fig. 3 shows variation of $P/(K_0T_2)$ with s_r for different θ. There exists a maximum for $P/(K_0T_2)$ as s_r varies, and the corresponding s_r is equal to 1. This suggests that the performance of FTEC is more excellent than that of ATEC from the perspective of $P/(K_0T_2)$. It is expected and the reasons are presented as follows. For $s_r < 1$, although much heat can be absorbed at the hot junction, the relatively small heat transfer area at the cold junction limits $P/(K_0T_2)$ of ATEC. And in the case of $s_r > 1$, since the absorbed heat at the hot junction is diminished compared to FTEC, $P/(K_0T_2)$ is also less than that of $s_r = 1$. This behavior can also be explained as: in the condition of constant Seebeck voltage (resulting from the constant temperatures of junctions T_1 and T_2), as the farther s_r is away from 1, the larger the electric resistance (Eq. (26)) is, hence, the lower $P/(K_0T_2)$ is. However, in some applications of heat source or heat sink with round shape [5,23–27], heat transfer capability between thermoelectric couple and heat source or heat sink is reduced considerably by geometries mismatching, provided that thermoelectric couple with suitable leg shape is not employed. Consequently, the performance of thermoelectric couple may be deteriorated seriously. This fact indicates that FTEC may not be the best choice in these applications and the selection of thermoelectric couple with proper leg shape is of great importance. Fig. 3 also shows that increasing θ does not affect the variation of $P/(K_0T_2)$ with s_r. For example, as s_r varies from 1.0 to 2.0, $P/(K_0T_2)$ is dropped by 2.6% for all considered θ.

Variation of η with s_r for different θ is shown in Fig. 4. s_r approximately has no effect on η in the studied case of $R_L/R_0 = 4.0$ and $ZT_m = 1.5$. This is attributed to the values of considered R_L/R_0 and those of R_L/R_0 for maximizing η. In detail, since the center section r_0 of n-type leg is considered as the dimensionless benchmark, R/R_0 has approximately the value of 2.0. According to Eq. (31), R_L/R_0 for maximizing η equals approximately to 3.2, which has no considerable difference with the considered R_L/R_0 ($R_L/R_0 = 4.0$). Therefore, in this situation, as shown in Eqs. (33) and (34), the influence of s_r on η is nearly negligible. This behavior between s_r and η disappears when R_L/R_0 deviates from the condition for maximizing η, which can be seen from Fig. 6.

Fig. 5 presents the variation of $P/(K_0T_2)$ with s_r under different R_L/R_0. A maximum of $P/(K_0T_2)$ is detected when equaling s_r to 1. Namely, FTEC outperforms than other typed thermoelectric couples with $s_r \neq 1$. This behavior is smeared out with increasing R_L/R_0. As the result presented in Eq. (30), Fig. 5 shows that the maximum of $P/(K_0T_2)$ occurs at $R_L/R_0 = 2.0$. The effect of s_r on η under different R_L/R_0 is given in Fig. 6, where some interesting results are found. Specifically, with $R_L/R_0 = 2.0$, as s_r increases, η increases before attaining a maximum after which it decreases, while this behavior reverses and a minimum of η emerges when $R_L/R_0 \geqslant 4.0$. The corresponding s_r for these extremums are $s_r = 1$. Besides, as long as R_L satisfies the condition shown in Eq. (31), η

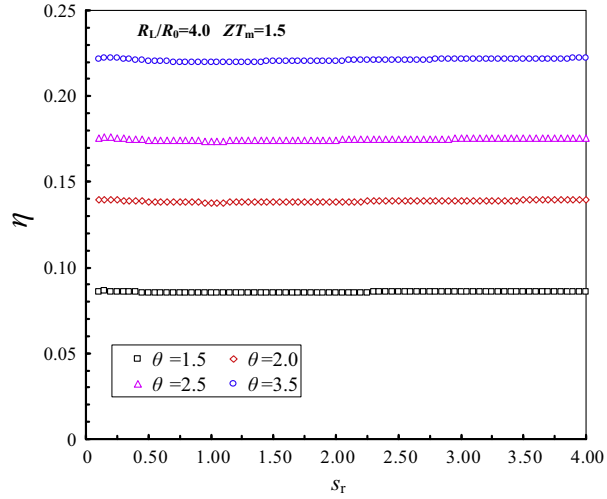

Fig. 4. Variation of η with s_r at different θ for $R_L/R_0 = 4.0$, $ZT_m = 1.5$.

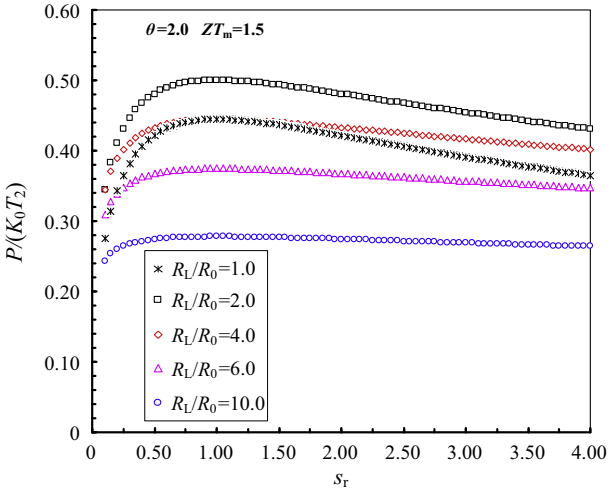

Fig. 5. Variation of $P/(K_0T_2)$ with s_r at different R_L/R_0 for $\theta = 2.0$, $ZT_m = 1.5$.

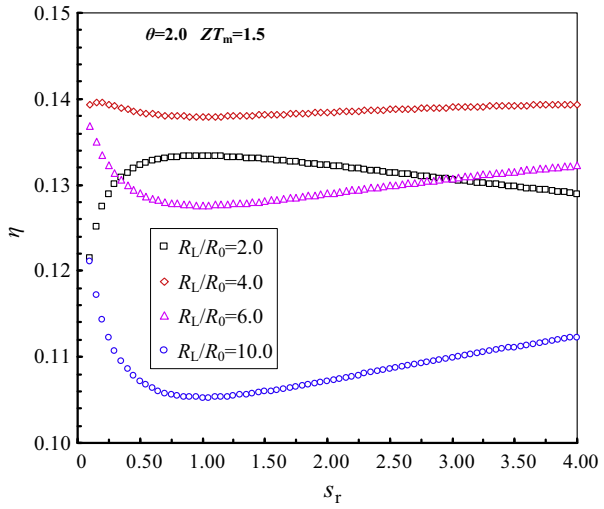

Fig. 6. Variation of η with s_r at different R_L/R_0 for $\theta = 2.0$, $ZT_m = 1.5$.

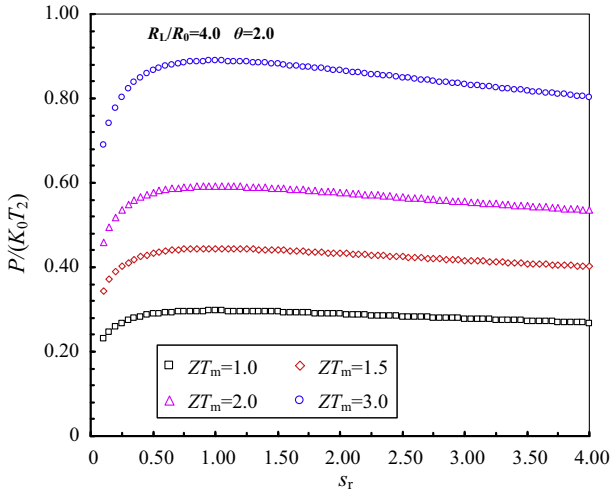

Fig. 7. Variation of $P/(K_0T_2)$ with s_r at different ZT_m for $R_L/R_0 = 4.0$, $\theta = 2.0$.

will reach the maximum regardless of s_r. These results imply that for practical applications of ATEC, much attention should be paid to the connected external load.

Figs. 7 and 8 show the variations of $P/(K_0T_2)$ and η with s_r for different ZT_m. Since the behaviors between $P/(K_0T_2)$ and s_r as well as between η and s_r are similar to those under different θ (shown in Figs. 3 and 4), the descriptions are not given in detail for the purposes of brevity.

To enhance the practicability of ATEC and to facilitate the practical applications, some suggestions or notes are provided.

(1) Above analysis indicates that compared to θ and ZT_m, the influence of s_r on the performance of ATEC is affected by R_L/R_0 seriously. Hence, enough attention should be paid to the external load matching when applying ATEC.

(2) Heat transfer capability between thermoelectric couple and heat source or heat sink, as a critical parameter for the performance of thermoelectric couple, is determined by both heat transfer coefficient and corresponding effective contacting area. Extensive work has been done mainly to enhance the heat transfer coefficient, while for effective contacting area, only little work has been done. Such a situation is probably understandable for flat-plate heat source or heat sink. However, in applications of heat source or heat sink with round shape [5,23–27], thermoelectric couple with suitable leg shape, i.e., ATEC, is obligatory to eliminate the heat transfer resistance caused by the geometries mismatching. Therefore, to improve the performance of thermoelectric couple, the effective contacting area (for instance, using thermoelectric couple in an appropriate shape) should be increased simultaneously with the increment of heat transfer coefficient.

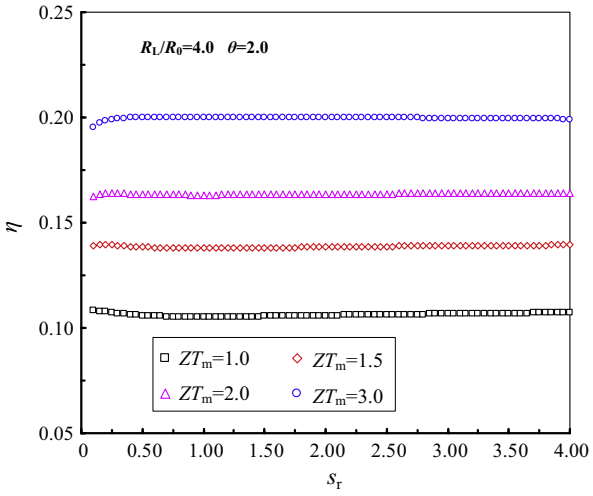

Fig. 8. Variation of η with s_r at different ZT_m for $R_L/R_0 = 4.0$, $\theta = 2.0$.

(3) Figs. 3, 5 and 7 show that the dimensionless power output of ATEC with $s_r = 1$ (FTEC) is higher than those with $s_r \neq 1$. Yet, previous analysis demonstrates that ATEC must be used for round shaped heat source or heat sink. Combining these two points as far as possible, a new structure presented in Fig. 9 is proposed for recovering cost-free energy resources, such as exhaust waste heat and solar energy. In this structure, an additive material with high thermal conductivity is employed between ATEC and round shaped heat source or heat sink. The advantages of this structure are listed as follows. Firstly, compared to previous structure without

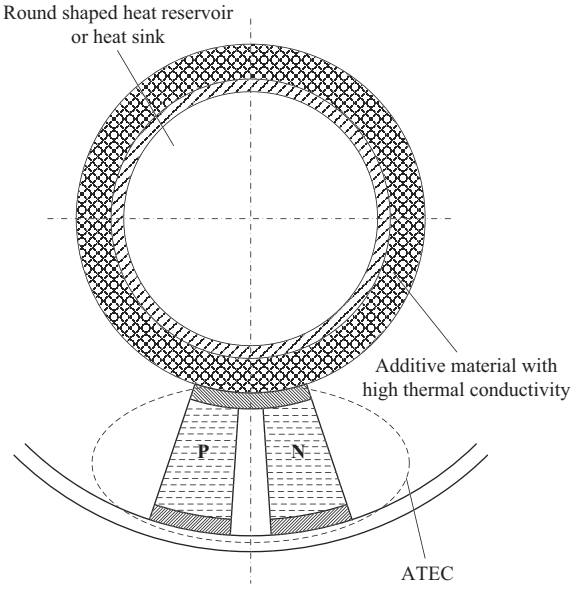

Fig. 9. Schematic of the proposed structure (only one ATEC is presented).

the additive material, s_r in this structure is more close to 1, and consequently ATEC in this structure has better performance. Also, the thermal stress is reduced, which can extend the lifetime of ATEC. Secondly, the effective contacting area, then heat transfer capability is increased compared to using FTEC. Consequently the performance of ATEC is improved. However, since an extra contacting surface between ATEC and round shaped heat source or heat sink is added by comparison to the previous structure without the additive material, care should be taken into account when using this structure.

4. Conclusions

To enhance heat transfer capability from the aspect of increasing effective contacting area, the annular thermoelectric couple (ATEC) is proposed for the practical applications with round shaped heat source or heat sink. An annular shaped parameter s_r is utilized to characterize ATEC. The fundamental formulas about ATEC are derived based on one-dimensional steady model. Theoretical analysis of the effect of s_r on the performance of ATEC under different temperature ratios, external loads and dimensionless figure of merits is carried out.

The results show that the fundamental formulas of ATEC are similar to those of flat-plate thermoelectric couple (FTEC) except for the expressions of overall thermal conductance and total electrical resistance. Specially, as s_r equals to 1, ATEC turns into FTEC. The extremums of dimensionless output power and efficiency are obtained when $s_r = 1$. The influence of s_r on the dimensionless output power and efficiency of ATEC is affected by the external load seriously as compared to the temperature ratio and dimensionless figure of merit. As external load increases, the extremum type of efficiency shifts from maximum to minimum. While for dimensionless output power, the type is always the maximum, but the effect of s_r becomes negligible. These imply that the selection of the external load for ATEC is of great importance. For generating power with cost-free energy resources, considering the fact that ATEC with $s_r = 1$ has higher dimensionless output power than those with $s_r \neq 1$, a new structure for ATEC is designed. In this structure, an additive material with high thermal conductivity between ATEC and round shaped heat source or heat sink is employed.

A more accurate theoretical model will be developed in the near future, in which the temperature-dependant properties of thermoelectric material, Thomson effect and non-adiabatic condition on lateral surface of ATEC legs will be considered.

Acknowledgment

This work was supported by the Fundamental Research Funds for the Central Universities (Project No. CDJZR13140014).

References

[1] Bell LE. Cooling, heating, generating power, and recovering waste heat with thermoelectric systems. Science 2008;321:1457–61.
[2] Chen G. Theoretical efficiency of solar thermoelectric energy generators. J Appl Phys 2011;109:104908-1–8-8.
[3] Fisac M, Villasevil FX, López AM. High-efficiency photovoltaic technology including thermoelectric generation. J Power Sources 2014;252:264–9.
[4] Hasan Nia M, Abbas Nejad A, Goudarzi AM, Valizadeh M, Samadian P. Cogeneration solar system using thermoelectric module and fresnel lens. Energ Convers Manage 2014;84:305–10.
[5] Crane D, LaGrandeur J, Jovovic V, Ranalli M, Adldinger M, Poliquin E, et al. TEG on-vehicle performance and model validation and what it means for further TEG development. J Electron Mater 2013;42:1582–91.
[6] Niu Z, Diao H, Yu S, Jiao K, Du Q, Shu G. Investigation and design optimization of exhaust-based thermoelectric generator system for internal combustion engine. Energ Convers Manage 2014;85:85–101.
[7] Zhao LD, Lo SH, Zhang Y, Sun H, Tan G, Uher C, et al. Ultralow thermal conductivity and high thermoelectric figure of merit in SnSe crystals. Nature 2014;508:373–7.
[8] Sahin AZ, Yilbas BS. The thermoelement as thermoelectric power generator: effect of leg geometry on the efficiency and power generation. Energ Convers Manage 2013;65:26–32.
[9] Ali H, Sahin AZ, Yilbas BS. Thermodynamic analysis of a thermoelectric power generator in relation to geometric configuration device pins. Energ Convers Manage 2014;78:634–40.
[10] Lesage FJ, Pelletier R, Fournier L, Sempels ÉV. Optimal electrical load for peak power of a thermoelectric module with a solar electric application. Energ Convers Manage 2013;74:51–9.
[11] Crane DT, Jackson GS. Optimization of cross flow heat exchangers for thermoelectric waste heat recovery. Energ Convers Manage 2004;45:1565–82.
[12] Gou X, Xiao H, Yang S. Modeling, experimental study and optimization on low-temperature waste heat thermoelectric generator system. Appl Energ 2010;87:3131–6.
[13] Chen WH, Liao CY, Hung CI, Huang WL. Experimental study on thermoelectric modules for power generation at various operating conditions. Energy 2012;45:874–81.
[14] Love ND, Szybist JP, Sluder CS. Effect of heat exchanger material and fouling on thermoelectric exhaust heat recovery. Appl Energ 2012;89:322–8.
[15] Wang Y, Dai C, Wang S. Theoretical analysis of a thermoelectric generator using exhaust gas of vehicles as heat source. Appl Energ 2013;112:1171–80.
[16] Jang JY, Tsai YC, Wu CW. A study of 3-D numerical simulation and comparison with experimental results on turbulent flow of venting flue gas using thermoelectric generator modules and plate fin heat sink. Energy 2013;53:270–81.
[17] Lesage FJ, Sempels ÉV, Lalande-Bertrand N. A study on heat transfer enhancement using flow channel inserts for thermoelectric power generation. Energ Convers Manage 2013;75:532–41.
[18] Amaral C, Brandão C, Sempels ÉV, Lesage FJ. Net thermoelectric generator power output using inner channel geometries with alternating flow impeding panels. Appl Therm Eng 2014;65:94–101.
[19] Wojtas N, Rüthemann L, Glatz W, Hierold C. Optimized thermal coupling of micro thermoelectric generators for improved output performance. Renew Energ 2013;60:746–53.
[20] Wang CC, Hung CI, Chen WH. Design of heat sink for improving the performance of thermoelectric generator using two-stage optimization. Energy 2012;39:236–45.
[21] Jang JY, Tsai YC. Optimization of thermoelectric generator module spacing and spreader thickness used in a waste heat recovery system. Appl Therm Eng 2013;51:677–89.
[22] Tzeng SC, Jeng TM, Lin YL. Parametric study of heat-transfer design on the thermoelectric generator system. Int Commun Heat Mass 2014;52:97–105.
[23] He W, Su Y, Riffat SB, Hou J, Ji J. Parametrical analysis of the design and performance of a solar heat pipe thermoelectric generator unit. Appl Energ 2011;88:5083–9.
[24] He W, Su Y, Wang YQ, Riffat SB, Ji J. A study on incorporation of thermoelectric modules with evacuated-tube heat-pipe solar collectors. Renew Energ 2012;37:142–9.
[25] Miljkovic N, Wang EN. Modeling and optimization of hybrid solar thermoelectric systems with thermosyphons. Sol Energy 2011;85:2843–55.
[26] Bauknecht A, Steinert T, Spengler C, Suck G. Analysis of annular thermoelectric couples with nonuniform temperature distribution by means of 3-D multiphysics simulation. J Electron Mater 2013;42:1641–6.
[27] Yazawa K, Hao M, Wu B, Silaen AK, Zhou CQ, Fisher TS, et al. Thermoelectric topping cycles for power plants to eliminate cooling water consumption. Energ Convers Manage 2014;84:244–52.
[28] <http://www.thermonamic.com/pro_view.asp?id=750> in 2014.
[29] Meng F, Chen L, Sun F. A numerical model and comparative investigation of a thermoelectric generator with multi-irreversibilities. Energy 2011;36:3513–22.
[30] Chen M, Rosendahl L, Bach I, Condra T, Pedersen J. Irreversible transfer processes of thermoelectric generators. Am J Phys 2007;75:815–20.
[31] Ren ZF, Chen G, Dresselhaus M. Nanostructured thermoelectric materials. In: Rowe DM, editor. Modules, systems, and applications in thermoelectrics. Boca Raton (London, NY): CRC Press; 2012. p. 1–2.